# Synthesis of Amphiphilic Pseudopolyamino Acid-Containing ABC-Triblock Copolymers and Micellar Characterizations

**Ren-Shen Lee,[1] Hua-Rong Li,[2] Fang-Chyou Chiu[2]**

[1]*Center of General Education, Chang Gung University, Kwei-Shan, Tao-Yuan, Taiwan, Republic of China*
[2]*Department of Chemical and Materials Engineering, Chang Gung University, Tao-Yuan, Taiwan, Republic of China*

Received 26 November 2008; accepted 2 August 2009
DOI 10.1002/app.31213
Published online 15 October 2009 in Wiley InterScience (www.interscience.wiley.com).

**ABSTRACT:** This study describes the synthesis of amphiphilic ABC-triblock copolymers comprising a central pseudopoly(4-hydroxy-L-proline) segment and terminal hydrophilic poly(ethylene glycol)methyl ether as well as hydrophobic poly(ε-caprolactone) blocks. Differential scanning calorimetry, $^1$H-NMR spectroscopy, and gel permeation chromatography are used to characterize the copolymers. The thermal properties ($T_g$ and $T_m$s) of the triblock copolymers depend on the composition of polymers. Larger amounts of ε-CL incorporated into the macromolecular backbone increased $T_g$ and $T_m$s. Fluorescence spectroscopy, transmission electron microscopy, and dynamic light scattering are utilized to investigate their micellar characteristics in the aqueous phase. Observations showed a higher critical micelle concentration with higher hydrophilic components in the copolymers. The micelle exhibited a core-shell-corona and/or vesicle shape, and the average size was less than 300 nm. Drug entrapment efficiency and drug loading of micelles depending on the composition of block polymers are also described. © 2009 Wiley Periodicals, Inc. J Appl Polym Sci 115: 2556–2564, 2010

**Key words:** amphiphilic; pseudopolyamino acid; MPEG-PHpr-PCL ABC-triblock copolymer; micelle

## INTRODUCTION

Block copolymers are the focus of intense research due to their ability to self-assemble into nanostructures with well-defined morphology and size. When a block copolymer is dissolved in a selective solvent, the insoluble (or less soluble) segments aggregate into dense micellar cores surrounded by coronas formed by the soluble blocks. Amphiphilic block copolymers with biocompatible and/or biodegradable sequences have potential applications in the biomedical field, e.g., as drug delivery systems and as gene therapy carriers. The ABC triblock copolymers have attracted great interest due to the (compared to AB and ABA block copolymers) huge number of different morphologies observed thus far in the bulk. Although many investigations have been performed on bulk ABC triblock copolymers during the last 20 years, preparing micelles with these copolymers is an emerging but promising field.[1,2]

Only a few biodegradable and/or biocompatible ABC triblock copolymers have been reported to date. Li and coworkers[3] reported synthesis and characterization of poly(ethylene glycol)-*b*-poly(ε-caprolactone)-*b*-poly(DL-lactide) triblock copolymers. Jing and coworkers[4–7] synthesized and characterized two kinds of triblock copolymers: RGD peptide-grafted poly(ethylene glycol)-*b*-poly(L-lactide)-*b*-poly(L-glutamic acid), and poly(ethylene glycol)-*b*-poly(L-lactide)-*b*-poly(L-lysine) with RGD peptide modification. Chen and coworkers[8,9] synthesized a novel structural triblock copolymer of poly(γ-benzyl-L-glutamic acid)-*b*-poly(ethylene oxide)-*b*-poly(ε-caprolactone) and cationic poly(ethylene glycol)-polyethylenimine-poly(γ-benzyl-L-glutamate) hyperbranched block copolymer. Contreras and coworkers[10] investigated novel ABC triblock copolymers with three potential crystallizable blocks: polyethylene (PE), poly(ethylene oxide) (PEO), and poly(ε-caprolactone) (PCL). Rzayev and Hillmyer[11] prepared nanoporous polystyrene containing hydrophilic pores from an ABC triblock copolymer polylactide-poly(*N*,*N*-dimethylacrylamide)-polystyrene (PLA-PDMA-PS). Bae and coworkers[12] investigated the pH-sensitive multifunctional poly(L-lactic acid)-*b*-poly(ethylene glycol)-*b*-poly(L-histidine) conjugate biotin polymeric micelle to enhanced tumor specificity. Recently, Börner and coworkers[13] reported the synthesis of amphiphilic ABC-triblock peptide-polymer conjugating a central

*Correspondence to:* R.-S. Lee (shen21@mail.cgu.edu.tw).
Contract grant sponsor: National Science Council; contract grant number: NSC 96-2221-E-182-023.
Contract grant sponsor: Chang Gung University; contract grant number: BMRP 123.

oligopeptide segment and terminal hydrophilic poly(ethylene oxide) (PEO) as well as hydrophobic poly(butyl acrylate) (PBA) blocks.

An earlier work of this study[14] reports the synthesis and micellar characterization amphiphilic ABA triblock copolymers based on hydrophilic dihydroxyl-terminated pseudo poly(*trans*-4-hydroxy-*N*-benzyloxycarbonyl-L-proline) (PNZHpr) macroinitiators (B block) and hydrophobic PCL (A block). This article describes the synthesis of amphiphilic ABC triblock copolymers comprising methoxy poly(ethylene glycol) (MPEG) for its hydrophilicity, nontoxicity, biocompatibility and nonimmunogenitity (A block), pseudo poly (*trans*-4-hydroxy-L-proline) (PHpr) in which hydroxyproline is a natural and major constituent of collagen (B block), and hydrophobic PCL for its biocompatible, biodegradable, and high permeability to drugs (C block). To our knowledge, the amphiphilic biodegradable and/or biocompatible MPEG-*b*-PHpr-*b*-PCL copolymers are the first being reported. This study investigates the micellar characteristics of these protected MPEG-*b*-PNZHpr-*b*-PCL and deprotected MPEG-*b*-PHpr-*b*-PCL triblock copolymers in the aqueous phase with fluorescence spectroscopy, dynamic light scattering (DLS), and transmission electron microscopy (TEM), and evaluates their potential as drug delivery systems.

## EXPERIMENTAL

### Materials

*Trans*-4-hydroxy-*N*-benzyloxycarbonyl-L-proline (NZHpr), MPEG 550 g $mol^{-1}$ (MPEG12, DP = 12), palladium-on-charcoal (10 wt %), pyrene, amitriptyline hydrochloride (AM) were purchased from Aldrich Chemical (Milwaukee, WI). Stannous octoate ($SnOct_2$) was purchased from Strem Chemical (Newburyport, MA). The ε-CL (Aldrich) was dried and vacuum-distilled over calcium hydride. In this work, organic solvents such as tetrahydrofuran (THF), methanol, chloroform, and *n*-hexane of high pressure liquid chromatography (HPLC) grade (Aldrich) were used as received Ultrapure water was used by purification with a Milli-Q Plus (Waters, Milford, MA).

### Synthesis of hydroxyl-terminated MPEG12-*b*-PNZHpr10 diblock copolymer

All glasses were dried in oven and handled under a dry nitrogen stream. The typical process for polymerization to give MPEG12-*b*-PNZHpr10 is as follows. MPEG12 ($M_n$ = 550 g $mol^{-1}$) (0.32 g, 0.57 mmol) and NZHpr (1.52 g, 5.73 mmol) were introduced into a flask and heated under a dry nitrogen stream to dissolve NZHpr. Then, 95 mg (5 wt %) of $SnOct_2$ was administered into the flask. The flask was purged with nitrogen and reacted at 170°C for 24 h. The resulting product was dissolved in $CHCl_3$, and then precipitated into excess *n*-hexane with stirring. The purified polymer was dried *in vacuo* at 50°C for 24 h and then analyzed. $^1$H-NMR and MALDI-TOF spectra of the MPEG12-*b*-PNZHpr10 are shown in Figures 1(A) and 2.

### Synthesis of MPEG12-*b*-PNZHpr10-*b*-PCL triblock copolymers

An amount of MPEG12-*b*-PNZHpr10 with hydroxyl end groups obtained above, with various molar ratios of ε-CL, and a dry stirring bar were put into a two-neck round-bottomed flask. In the presence of $SnOct_2$ (1.5 wt % based on the weight of MPEG12-*b*-PNZHpr10 and ε-CL) as the catalyst, the polymerization was initiated at 110°C under a dry nitrogen stream for 24 h. The resulting product was dissolved in $CHCl_3$, and was then precipitated into excess *n*-hexane with stirring. The purified polymer was dried *in vacuo* at 50°C for 24 h and then analyzed. Representative $^1$H-NMR and FTIR spectra of the MPEG12-*b*-PNZHpr10-*b*-PCL110 are shown in Figures 1(B) and 3(B).

### Deprotection of the benzyloxycarbonyl-protecting group of new copolymer

A 10 wt % palladium-on-charcoal catalyst (1 g) was added to a 10 mL solution of the MPEG12-*b*-PNZHpr10-*b*-PCL70 (0.5 g) whose amino groups were protected by benzyloxycarbonyl (Z) in THF/$CH_3OH$ (v/v = 1/1). After purging with nitrogen three times, the reaction mixture was stirred under 1.0 atm hydrogen pressure at 50°C for 3 days. After the deprotection reaction, the catalyst was removed by filtration, and the solution was concentrated to approximately one-fourth the volume under reduced pressure. The concentrated solution was poured into *n*-hexane to precipitate, and the deprotected polymer MPEG12-*b*-PHpr10-*b*-PCL70 was obtained and then analyzed by $^1$H-NMR and FTIR. The $^1$H-NMR and IR spectra of MPEG12-*b*-PHpr10-*b*-PCL70 are shown in Figures 1(C) and 3(A).

### Characterization

$^1$H-NMR spectra were obtained on a Bruker WB/DMX-500 spectrometer (Ettlingen, Germany) at 500 MHz with chloroform (δ = 7.24 ppm) as an internal standard and in $CDCl_3$. The IR spectra were measured on a Bruker TENSOR 27 Fourier transform infrared (FTIR) spectrophotometer (Bruker, Germany). Samples were either neatly placed on NaCl

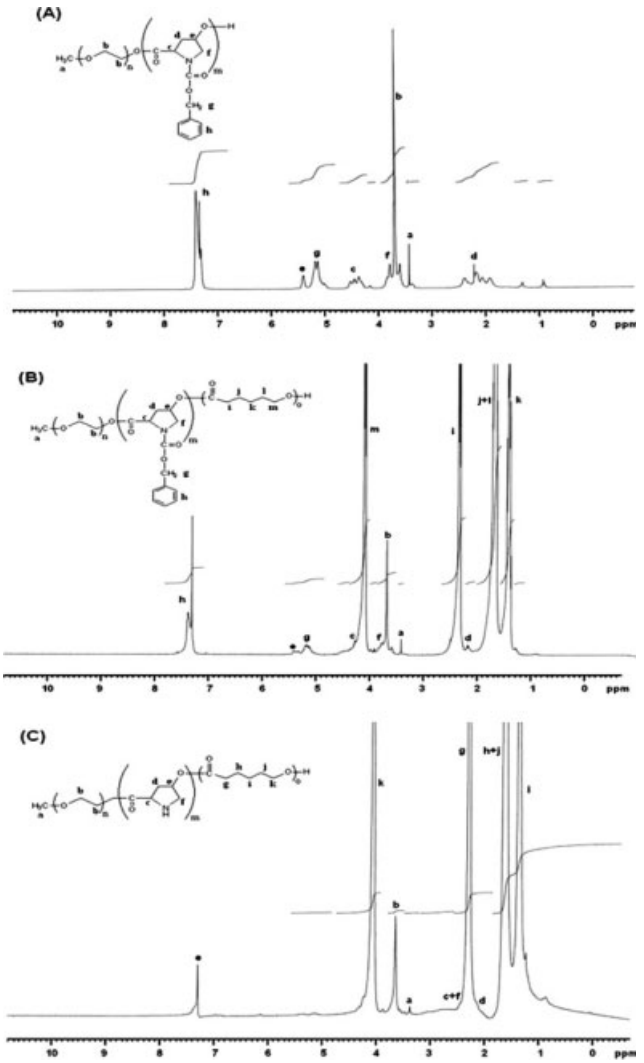


**Figure 1** Representative $^1$H-NMR spectra of (A) MPEG12-*b*-PNZHpr10 diblock copolymer, (B) MPEG12-*b*-PNZHpr10-*b*-PCL110, and (C) deprotected MPEG12-*b*-PHpr10-*b*-PCL110 triblock copolymer in $CDCl_3$.

plates or pressed into KBr pellets. A thermal analysis of the polymer was performed on a DuPont 9900 system, consisting of DSC (Newcastle, DE). The heating rate was 20°C min$^{-1}$. The $T_g$s were read at mid-change in heat capacity and taken from the second heating scan after quick cooling. A GPC system determined the number-average molecular weight ($M_n$) and weight-average molecular weights ($M_w$), of the polymer, respectively. It was carried out on a Jasco HPLC system equipped with a model PU-2031 refractive-index detector (Tokyo, Japan), and Jordi Gel polydivinyl benzene (DVB) columns with pore sizes of 100, 500, and 1000 Å. Chloroform was used as the eluent at a flow rate of 0.5 mL min$^{-1}$. Polystyrene standards with a low dispersity (Polymer Sciences) generated a calibration curve. Windows-based software package (Scientific

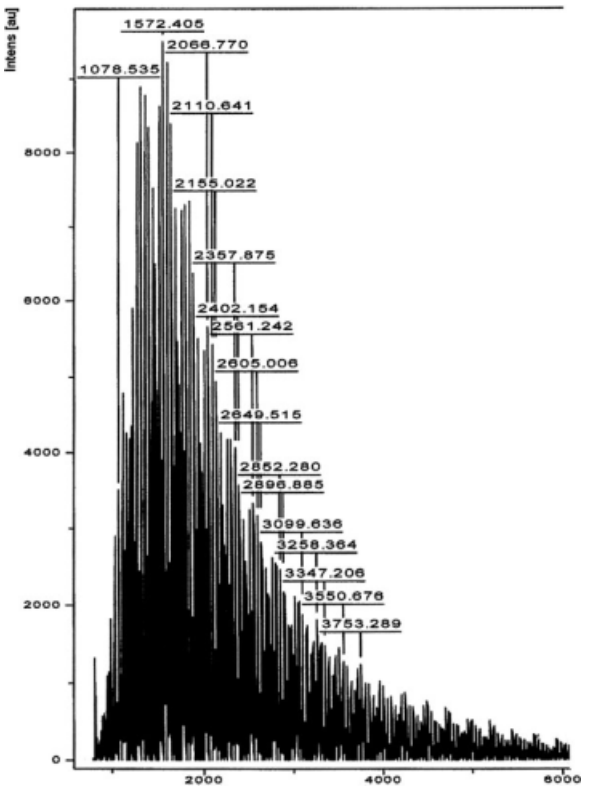


**Figure 2** MALDI-TOF spectrum for macroinitiator MPEG12-*b*-PNZHpr10.

Information Service Co.) was used to record and manipulate the data.

The matrix-assisted laser desorption/ionization time-of-flight (MALDI-TOF) mass spectrometry analysis were performed on an Ultraflex MALDI-TOF/TOF mass spectrometer (Bruker Daltonik GmbH, Bremen, Germany). The mass range from 600 to 7000 *m/z* was recorded in positive-ion reflection mode. Typically, 0.5 μL of the sample was dried on a target plate (600-μm AnchorChip, Bruker Daltonics) and cocrystallized with 0.3 μL of a matrix

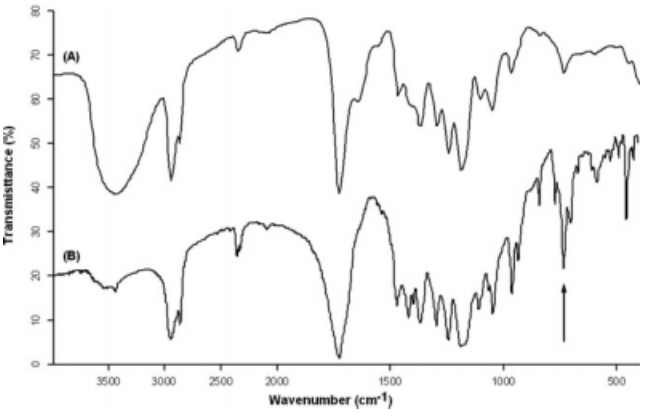


**Figure 3** FTIR spectra of (A) MPEG12-*b*-PHpr10-*b*-PCL70 and (B) MPEG12-*b*-PNZHpr10-*b*- PCL70.

solution (2 mg $mL^{-1}$ α-cyano-4-hydroxycinnamic acid in 80% acetonitrile and 1% trifluoroacetic acid) containing 3 fmol of purified peptides from anti-bovine albumin (BSA) (clip 161–167, *m/z* 927.49), α-s2-casein (clip 130–140, *m/z* 1195.68) and adrenocorticotropic hormone (ACTH) (clip18–39, *m/z* 2465.20). The samples were then irradiated with a nitrogen laser (337 nm) with an accelerating voltage of 25 kV and a delay of 200 ns. Typically, the experiment accumulated data from 200 to 500 laser shots to obtain acceptable quality. The spectra were calibrated internally with the introduced peptides.

Ultraviolet-visible (UV–vis) spectra were obtained with a Jasco V-550 spectrophotometer (Tokyo, Japan). The pyrene fluorescence spectra were recorded on a Hitachi F-4500 spectrofluorometer (Japan). Square quartz cells ($1.0 \times 1.0$ $cm^2$) were used. For fluorescence excitation spectra, the detection wavelength ($\lambda_{em}$) was set at 390 nm.

### Measurements of fluorescence spectroscopy

To prove micelles formation, fluorescence measurements were carried out using pyrene as a probe.[15] Fluorescence spectra of pyrene in aqueous solution were recorded at room temperature on a fluorescence spectrophotometer. The sample solutions were prepared by first adding known amounts of pyrene in acetone to a series of flasks. After the acetone evaporated completely, measured amounts of micelle solutions with various concentrations of MPEG12-*b*-PNZHpr10-*b*-PCL30 (75, 37.5, 18.75, 9.38, 4.69, and 2.34 mg $L^{-1}$) were added to each of the flasks and mixed via vortexing. Pyrene concentration in the final solutions was $6.1 \times 10^{-7}$ M. The flasks were allowed to stand overnight at room temperature to equilibrate the pyrene and the micelles. For fluorescence excitation spectra, the detection wavelength ($\lambda_{em}$) was set at 390 nm.

### Preparation of polymeric micelles

Polymeric micelles of MPEG12-*b*-PNZHpr10-*b*-PCL copolymers were prepared using the oil-in-water (o/w) emulsion technique. Briefly, 30 mg of each polymer was dissolved in dichloromethane (MC, 5 mL). The solution was added dropwise into DI water (100 mL) with vigorous stirring at ambient temperature. Then, the emulsion solution was ultrasonic for 1 h and stirred at ambient temperature for overnight. After the MC was completely evaporated, obtain a polymeric micelles solution.

### Measurements of size and size distribution

The size distribution of micelles were estimated by a DLS using a Particle-Size Analyzer (Zetasizer nano ZS, Malvern, UK) at 20°C. Scattered light intensity was detected at 90° to an incident beam. Measurements were made after filtering the aqueous micellar solution ($C = 0.3$ g $L^{-1}$) with a microfilter having an average pore size of 0.2 μm (Advantec MFS, USA). An average size distribution of aqueous micellar solution was determined based on CONTIN programs of Provencher and Hendrix.[16]

### Observation on transmission electron microscope

Micelle morphology was observed by TEM (JEM 1200-EXII, Tokyo, Japan). Drops of micelle solution ($C = 0.3$ g $L^{-1}$, containing no stain agent) were placed on a carbon film-coated copper grid, and then dried at room temperature. Observation was done at an accelerating voltage of 100 kV.

### Determination of drug-loading content and drug entrapment efficiency

Using oil-in-water emulsion, solvent evaporation method, MPEG12-*b*-PNZHpr10-*b*-PCL (50-fold CMC value) was dissolved in 6 mL methylene chloride followed by adding antidepressant drug amitriptyline hydrochloride (AM) with various weight ratios to the polymer (1/10–1/1) serving as a model drug. The solution was added dropwise to 150 mL distilled water under vigorous stirring. Droplet size was reduced by sonication at ambient temperature for 60 min. The emulsion was stirred at ambient temperature overnight to evaporate the methylene chloride. The aggregated AM-loaded micelles were removed by centrifugation (3000 rpm × 30 min). Then, the aqueous micelles solution was dried at room temperature with a vacuum rotary evaporator. As AM water solubility is much more than the block copolymer and micelle, the unloaded AM was eliminated by washing three times with distilled water. The micelles were obtained by vacuum drying. A weighed amount of micelle was disrupted by adding acetonitrile (10 mL). Drug content was assayed spectrophotometrically at 240 nm using a Diode Array UV-vis Spectrophotometer. Equations (1) and (2) calculate drug-loading content and drug entrapment efficiency, respectively:

$$\text{Drug-loading content (\%)} = (\text{weight of drug in micelles/weight of micelles}) \times 100 \quad (1)$$

$$\text{Drug entrapment efficiency (\%)} = (\text{weight of drug in micelles/weight of drug fed initially}) \times 100 \quad (2)$$

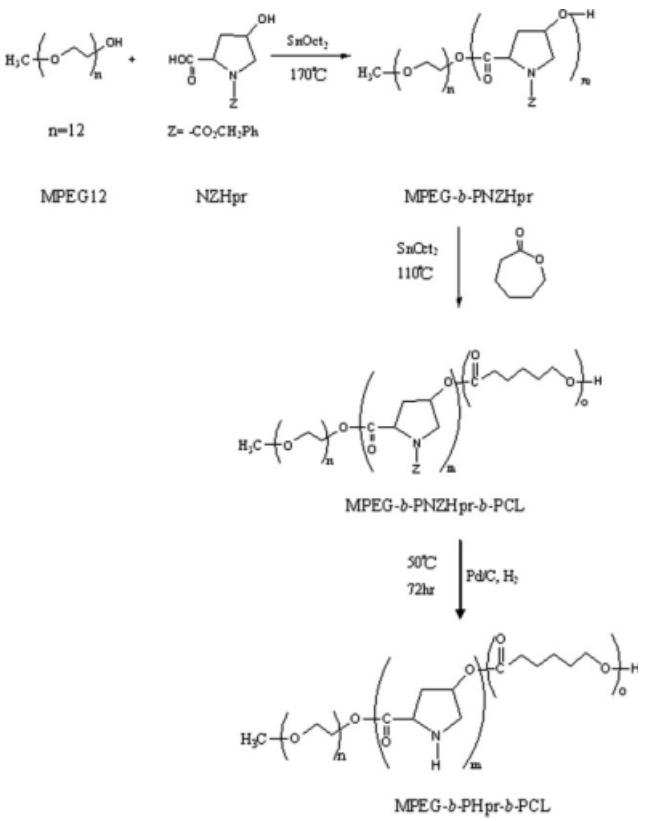


**Scheme 1** Synthesis of the MPEG-*b*-PHpr-*b*-PCL triblock copolymer.

## RESULTS AND DISCUSSION

### Synthesis and characterization of the MPEG12-*b*-P(NZ)Hpr10-*b*-PCL

This work performed on various MPEG12-*b*-PNZHpr10-*b*-PCL triblock copolymers via ring-opening polymerization of ε-CL with hydroxyl-terminated diblock macroinitiator MPEG12-*b*-PNZHpr10. Scheme 1 illustrates the synthesis of amphiphilic MPEG12-*b*-PNZHpr10-*b*-PCL triblock copolymers. The experiment first prepared hydroxyl-terminated MPEG12-*b*-PNZHpr10 by polycondensation of NZHpr and initiator MPEG12 (with a molar ratio of 10/1) in the presence of $SnOct_2$ (5 wt %) as the catalyst in bulk at 170°C for 24 h. The primary hydroxyl group of MPEG was more reactive than the secondary hydroxyl group of NZHpr in polymerization. The prepared MPEG12-*b*-PNZHpr10 macroinitiator was characterized by GPC ($M_n$ = 1470, $M_w/M_n$ = 1.53); MALDI-TOF mass spectroscopy ($M_n$ = 1572) (Fig. 2) and $^1$H-NMR spectroscopy [Fig. 1(A)]. The hydroxyl group of MPEG12-*b*-PNZHpr10 were used as initiation sites for ring-opening polymerization of ε-CL with $SnOct_2$ as the catalyst to produce MPEG12-*b*-PNZHpr10-*b*-PCL triblock copolymers, with the fixed MPEG12-*b*-PNZHpr10 macroinitiator, copolymers with different compositions were prepared by making changes in the monomer ε-CL feed ratios for $SnOct_2$-catalyzed polymerization at 110°C for 24 h. Table I lists the results of the polymerization with moderate yields. The triblock copolymers $M_n$ values increased as the molar ratios of ε-CL to MPEG12-*b*-PNZHpr10 increased in the feed. The $M_n$ values of the copolymers increased from 5440 to 12,790 g mol$^{-1}$, with $M_w/M_n$ between 1.35 and 1.89; the molar ratios of ε-CL to MPEG12-*b*-PNZHpr10 in the feed increased from 30 to 110. The molar ratios of compositions in the block copolymers were analyzed with $^1$H-NMR. Monomer amounts incorporated into the copolymer were calculated from comparing the integral area of resonance peaks (δ = 3.39 ppm) of terminal methoxy protons of MPEG12-*b*-PNZHpr10 with resonance peaks (δ = 1.64 ppm) of the $C_3$ and $C_5$ methylene protons of PCL. Converting copolymerization of the ε-CL was systematically higher than the corresponding feeds because of its high reactivity in polymerization. However, there

**TABLE I**
**Results of the Block Copolymerization of ε-Caprolactone Initiated with MPEG12-*b*-PNZHpr10 in Bulk at 110°C with $SnOct_2$ (1.5 wt %) as the Catalyst for 24 h**

| Copolymers | Molar ratio of ε-CL over MPEG12-*b*-PNZHpr10 in Feed[a] | Molar ratio of ε-CL over MPEG12-*b*-PNZHpr10 determined by $^1$H-NMR | Yield (%) | $M_{n,GPC}$ | $M_{n,calcd}$[b] | $M_{n,NMR}$[c] | $M_w/M_n$[d] | $T_g$[e] (°C) | $T_m$[e] (°C) |
|---|---|---|---|---|---|---|---|---|---|
| MPEG12-*b*-PNZHpr10-*b*-PCL110 | 110 : 1 | 174 : 1 | 67 | 12,790 | 14,010 | 21,310 | 1.35 | −46.6 | 54.6, 51.0 |
| MPEG12-*b*-PNZHpr10-*b*-PCL90 | 90 : 1 | 135 : 1 | 57 | 9,900 | 11,730 | 16,860 | 1.71 | −47.1 | 54.1, 49.3 |
| MPEG12-*b*-PNZHpr10-*b*-PCL70 | 70 : 1 | 84 : 1 | 48 | 9,550 | 9,140 | 11,040 | 1.65 | −47.8 | 53.8, 49.3 |
| MPEG12-*b*-PNZHpr10-*b*-PCL50 | 50 : 1 | 44 : 1 | 66 | 7,030 | 7,170 | 6,480 | 1.63 | −48.5 | 52.7, 49.4 |
| MPEG12-*b*-PNZHpr10-*b*-PCL30 | 30 : 1 | 41 : 1 | 55 | 5,440 | 4,890 | 6,140 | 1.89 | −50.3 | 52.5, 48.9 |

[a] $M_n$ of MPEG12-*b*-PNZHpr10: 1470 g mol$^{-1}$.
[b] $M_{n,calcd} = M_{n,MPEG12\text{-}b\text{-}PNZHpr10}$ + [ε-CL]/[MPEG12-*b*-PNZHpr10] × 114.
[c] $M_{n,NMR}$ is determined by $^1$H-NMR spectroscopy of MPEG12-*b*-PNZHpr10-*b*-PCL.
[d] Number-average molecular weight ($M_n$) and weight-average molecular weight ($M_w$) are determined by GPC.
[e] Determined from DSC thermograms at 20°C min$^{-1}$.

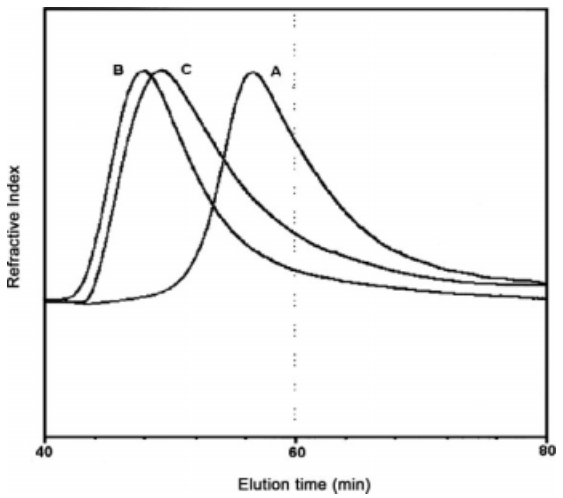


**Figure 4** GPC curves of (A) AB diblock copolymer MPEG12-*b*-PNZHpr10, (B) ABC triblock copolymer MPEG12-*b*-PNZHpr10-*b*-PCL70, and (C) deprotected ABC triblock copolymer MPEG12-*b*-PHpr10-*b*-PCL70.

was good agreement between the theoretical molar weight ($M_{n,\mathrm{th}}$) and the GPC-determined number-average molecular weight ($M_{n,\mathrm{GPC}}$). Figure 1(B) shows the typical $^1$H-NMR spectrum of the triblock copolymer MPEG12-*b*-PNZHpr10-*b*-PCL110 with a molar ratio of [ε-CL]/[MPEG12-*b*-PNZHpr10] = 174. The peaks are assigned to the corresponding hydrogen atoms of the copolymers. The secondary hydroxyl proton signal at δ = 3.31 ppm for the original MPEG12-*b*-PNZHpr10 macroinitiator disappeared. This demonstrated that the MPEG12-*b*-PNZHpr10 macroinitiator completely initiated ε-CL polymerization to form the block copolymer within NMR detection limits. Figure 4 shows typical GPC curves of the triblock copolymers compared with those of the original MPEG12-*b*-PNZHpr10 macroinitiator. The GPC traces show a unimodal distribution of the block copolymer and do not show the presence of any possible homopolymerized PCL. In each block copolymer, the peak shifted toward a higher molecular weight region compared with the peak of the original MPEG12-*b*-PNZHpr10 macroinitiator, with little change in molecular weight distribution. These preliminary results show that block copolymerization of the hydroxyl-group terminated the MPEG12-*b*-PNZHpr10 macroinitiator and ε-CL using the $SnOct_2$-catalyst was successful under the experimental conditions. Representative FTIR spectrum of the triblock copolymer MPEG12-*b*-PNZHpr10-*b*-PCL70 with a molar ratio of [ε-CL]/[MPEG12-*b*-PNZHpr10] = 70 is shown in Figure 3(B). The major absorption peaks of MPEG12-*b*-PNZHpr10-*b*-PCL70 at 2950 (C—H), 1740 (carbonyl), and 740 cm$^{-1}$ (aromatic C—H) were observed.

The benzyloxycarbonyl protective groups of MPEG12-*b*-PNZHpr10-*b*-PCL can be removed by catalytic-transfer hydrogenation. The deprotection of MPEG12-*b*-PNZHpr10-*b*-PCL70 is confirmed with $^1$H-NMR and FTIR as shown in Figures 1(C) and 3(A). From the $^1$H-NMR spectrum, the proton signals of benzyloxycarbonyl (δ = 5.12, and 7.34 ppm) are almost disappeared. Compared with the IR spectrum of the benzyl protected copolymers as shown in Figure 3(B), the most distinctive features of deprotected MPEG12-*b*-PHpr10-*b*-PCL70 were the almost complete absence of aromatic C—H (out-of-plane bending) vibration absorption at 699 and 750 cm$^{-1}$ from the benzyl protected group and a broad amino vibration band at 3480 cm$^{-1}$. This indicated the successful removal of the benzyloxycarbonyl group. Figure 4(C) shows GPC trace of the deprotected polymer. Compared to that of MPEG12-*b*-PNZHpr10-*b*-PCL70 [Fig. 4(B)], its peak shifted to the lower molecular weight side due to removing the protecting groups, as and its $M_w/M_n$ remains unchanged. This implies negligible main-chain degradation of the polymer. Table I and Figure 5 show thermal behaviors of the block copolymers and DSC curves of MPEG12-*b*-PNZHpr10-*b*-PCL. According to DSC, observations show increased $T_g$ and $T_m$s of the copolymers with increased contents of ε-CL incorporated into the copolymers. The values of $T_g$ and $T_m$s increased from −50.3° to −46.6°, and from 48.9 to 51.0 and 52.5 to 54.6°C, respectively, when the [ε-CL]/[MPEG12-*b*-PNZHpr10] molar ratios increased from 41 to 174. This was due to the fact that copolymers have higher molecular weight: when larger amounts of ε-CL were incorporated into the macromolecular backbone, $T_g$ and $T_m$s increased. The existence of two melting temperature very close together might be the primary and secondary crystallization of PCL. But, the

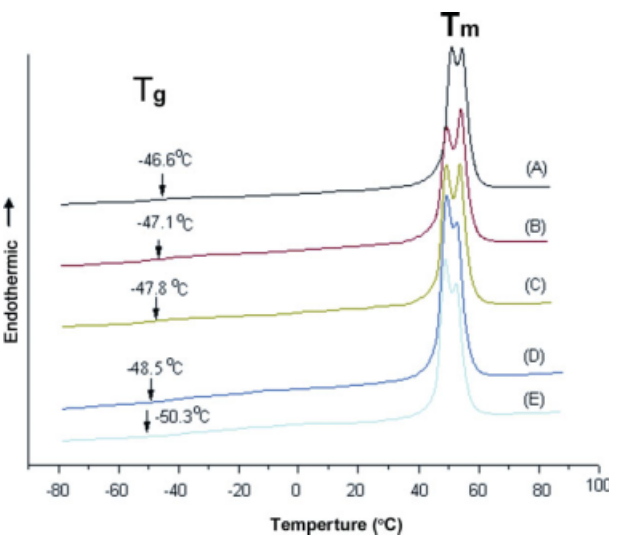


**Figure 5** DSC curves of MPEG12-*b*-PNZHpr10-*b*-PCL with the molar ratios [ε-CL]/[MPEG12-*b*-PNZHpr10] (A) 174/1, (B) 135/1, (C) 84/1, (D) 44/1, (E) 41/1 for second run. [Color figure can be viewed in the online issue, which is available at www.interscience.wiley.com.]

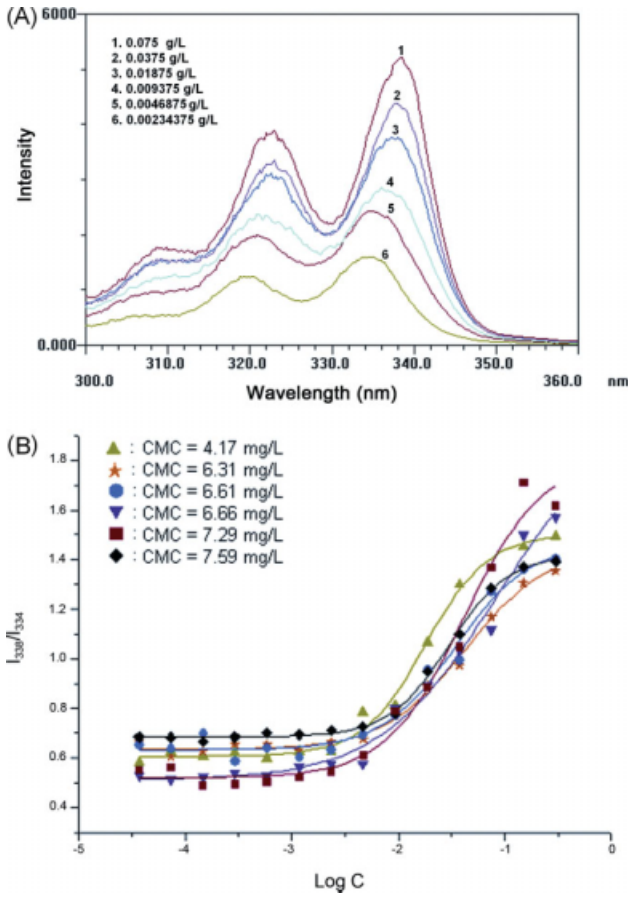


**Figure 6** (A) Excitation spectra of the MPEG12-*b*-PNZHpr10-*b*-PCL30 copolymer monitored at $\lambda_{em} = 390$ nm and (B) plot of the $I_{338}/I_{334}$ intensity ratio (from pyrene excitation spectra, pyrene concentration $= 6.1 \times 10^{-7}$ M) versus the logarithm of the concentration (log *C*) for (▲, bright green) MPEG12-*b*-PNZHpr10-*b*-PCL110, (★, light orange) MPEG12-*b*-PNZHpr10-*b*-PCL90, (●, blue) MPEG12-*b*-PNZHpr10-*b*-PCL70, (▼, violet) MPEG12-*b*-PNZHpr10-*b*-PCL50, (■, red) MPEG12-*b*-PNZHpr10-*b*-PCL30, and (◆, black) MPEG12-*b*-PHpr10-*b*-PCL70 triblock copolymers ($\lambda_{em} = 390$ nm). [Color figure can be viewed in the online issue, which is available at www.interscience. wiley.com.]

$T_m$ of the copolymers were slightly lower than the PCL ($T_m = 58.3°C$),[17] indicating that the presence of MPEG12-*b*-PNZHpr10 blocks decreased crystallinity of the copolymer with respect to the PCL homopolymer by reducing PCL chain mobility.

### Micelles of block copolymers

The amphiphilic nature of the triblock copolymers, consisting of hydrophilic block MPEG, and two hydrophobic blocks PNZHpr as well as PCL, provided an opportunity to form micelles in water. This work investigated characteristics of the triblock copolymer micelles in an aqueous phase with fluorescence techniques. The critical micelle concentration (CMC) values of the triblock copolymers in an aqueous phase were determined by a fluorescence technique with pyrene as a probe.[15]

Figure 6(A) shows excitation spectra of pyrene in MPEG12-*b*-PNZHpr10-*b*-PCL30 solutions with various concentrations. The fluorescence intensity increased with increasing concentration of MPEG12-*b*-PNZHpr10-*b*-PCL30. The characteristic pyrene excitation spectra, a redshift of the (0, 0) band from 334 to 338 nm upon pyrene partitioning into the micellar hydrophobic core, was used to determine CMC values of the MPEG12-*b*-PNZHpr10-*b*-PCL triblock copolymers. Figure 6(B) shows intensity ratios ($I_{338}/I_{334}$) of pyrene excitation spectra versus the logarithm of the MPEG12-*b*-PNZHpr10-*b*-PCL110–30 and deprotected MPEG12-*b*-PHpr10-*b*-PCL70 triblock copolymer concentrations. As the copolymer concentration increased, at a certain concentration (i.e., the CMC), the value of $I_{338}/I_{334}$ increased dramatically in a sigmoid manner. The CMC was determined from intersecting straight line segments drawn through points at the lowest polymer concentrations, which lay on a nearly horizontal line, with that going through points on the rapidly rising part of the plot. The CMC values of the triblock copolymers MPEG12-*b*-PNZHpr10-*b*-PCL110∼30 increased from 4.17 to 7.29 mg $L^{-1}$, with decreasing of hydrophobic PCL chain length. The CMC values were much lower than those of low-molecular-weight surfactants (e.g., 2.3 g $L^{-1}$ for sodium dodecyl sulfate in water) and were comparable with those of other polymeric amphiphiles.[4] As the MPEG12-*b*-PNZHpr10-*b*-PCL70 was deprotected, CMC values of the copolymer increased from 6.61 to 7.59 mg $L^{-1}$. This demonstrated increased hydrophilicity when the protecting groups of PNZHpr were deprotected.

The mean hydrodynamic diameters of micelles from DLS were in the range of 120–300 nm, and size distribution showed a monodisperse unimodel pattern as shown in Figure 7. The results indicated that micelles size were dependent on polymer composition. Fixing the concentration at 50-fold CMC (50 × CMC) value, micelles size increases with increased ratio of the hydrophobic segment to the hydrophilic segment in copolymer. Micelle size of the deprotected MPEG12-*b*-PHpr10-*b*-PCL70 (pH = 3.53) was bigger than that of the protected MPEG12-*b*-PNZHpr10-*b*-PCL70, which may attribute to the electrostatic repulsion of ammonium groups after deprotecting. Compared to sizes of loaded and unloaded AM drug micelles, the size decreased when AM was loaded in MPEG12-*b*-PHpr10-*b*-PCL micelle (Fig. 8). We assume that the AM-loaded reduced the electrostatic repulsion of ammonium groups, resulting in constriction of the core. Observations showed a similar result on TEM morphology. Figure 9 shows micelle morphology formed by MPEG12-*b*-PNZHpr10-*b*-PCL. The images confirm that the copolymers

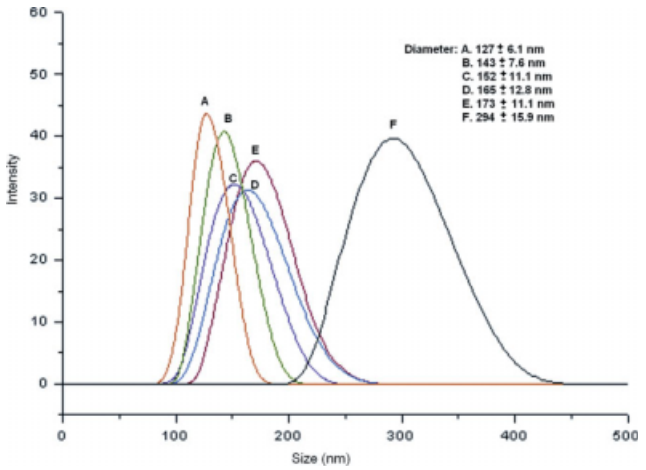


**Figure 7** Effect of composition of MPEG12-*b*-PNZHpr10-*b*-PCL with the molar ratios [ε-CL]/[MPEG12-*b*-PNZHpr10] (A) 41/1, (B) 44/1, (C) 84/1, (D) 135/1, (E) 174/1, and (F) deprotected C on the size of micelle particles at the 50-fold CMC (50 × CMC) value. [Color figure can be viewed in the online issue, which is available at www.interscience.wiley.com.]

formed almost core-shell-corona shapes. However, the vesicle shape was observed after deprotecting.

### Drug-loading content and drug entrapment efficiency

This study selected the antidepressant drug AM as a model drug. Table II summarizes the drug-loading content and drug entrapment efficiency of MPEG12-*b*-PNZHpr10-*b*-PCL110–30 and MPEG12-*b*-PHpr10-*b*-PCL triblock copolymeric micelles. The drug-loading content and drug entrapment efficiency depended mainly on copolymer composition and the feed weight ratio of AM to the polymer. For protected MPEG12-*b*-PNZHpr10-*b*-PCL70 and deprotected MPEG12-*b*-PHpr10-*b*-PCL70, as the feed weight ratio of AM to the polymer increased from 0.1 to 1, drug entrapment efficiency decreased from 17.6 to 2.4% and from 12.0 to 3.0%, respectively. This may be due to entrapment amount of the drug being limited. Therefore, as the weight of drug fed initially [denominator of eq. (2)] increased, resulted entrapment efficiency decreased. But, our finding show disagreement changes with

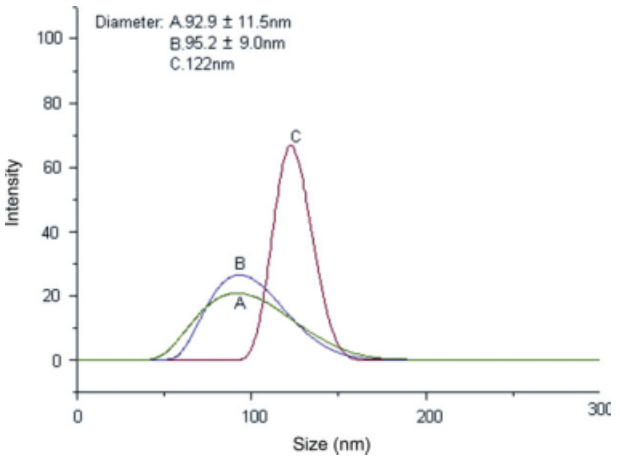


**Figure 8** AM loaded particle size distribution of MPEG12-*b*-PNZHpr10-*b*-PCL with the different length of PCL block (A) PCL50, (B) PCL70, and (C) PCL110. [Color figure can be viewed in the online issue, which is available at www.interscience.wiley.com.]

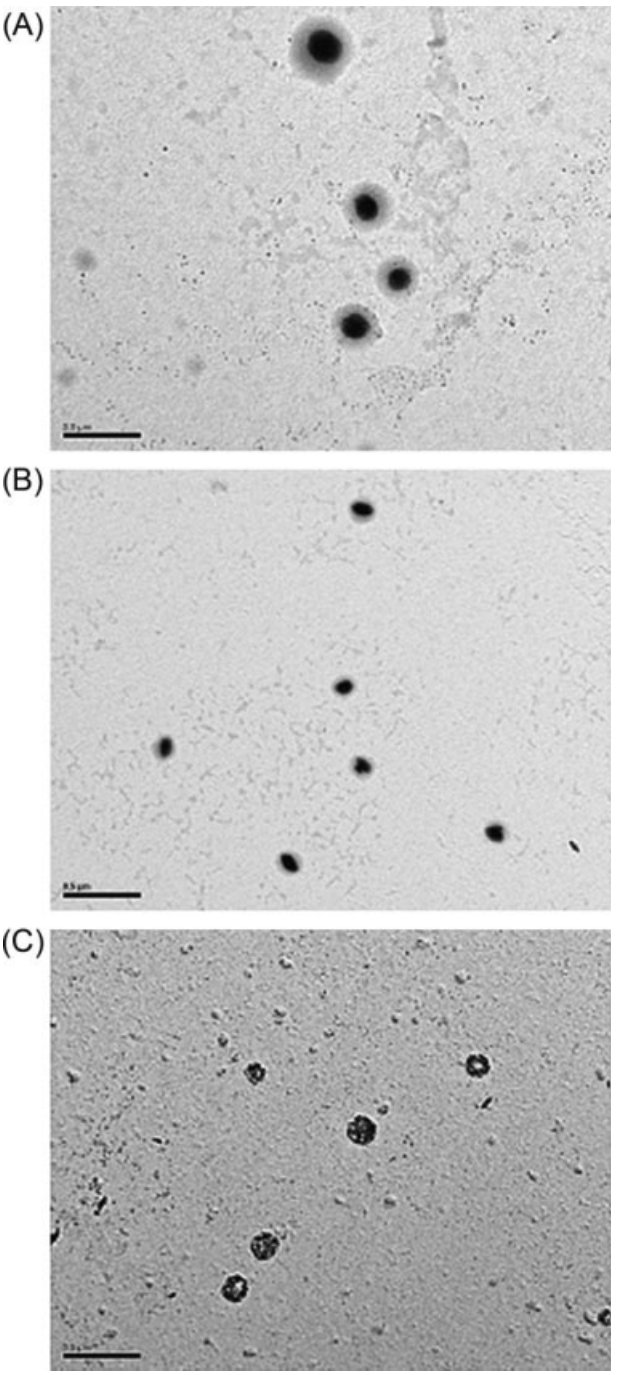


**Figure 9** Representative TEM photograph of the micelles formed by the (A) MPEG12- *b*-PNZHpr10-*b*-PCL110, (B) MPEG12-*b*-PNZHpr10-*b*-PCL110 loading with AM, (C) deprotected MPEG12-*b*-PHpr10-*b*-PCL70 (scale bar = 500 nm).

**TABLE II**
**Drug Entrapment Efficiency and Drug Loading of AM-Loaded MPEG12-*b*-P(NZ)Hpr10-*b*-PCL Triblock Copolymer Micelles**

| Copolymers | Feed weight ratio (AM/polymer) | Drug entrapment efficiency (%) | Drug loading (%) |
|---|---|---|---|
| MPEG12-*b*-PNZHpr10-*b*-PCL70 | 1/10 | 17.6 ± 0.99 | 2.1 ± 0.07 |
| MPEG12-*b*-PNZHpr10-*b*-PCL70 | 1/4 | 7.2 ± 0.36 | 2.2 ± 0.23 |
| MPEG12-*b*-PNZHpr10-*b*-PCL70 | 1/2 | 3.9 ± 0.08 | 2.3 ± 0.48 |
| MPEG12-*b*-PNZHpr10-*b*-PCL70 | 1/1 | 2.4 ± 0.07 | 4.6 ± 1.00 |
| MPEG12-*b*-PHpr10-*b*-PCL70 | 1/10 | 12.0 | 8.6 |
| MPEG12-*b*-PHpr10-*b*-PCL70 | 1/4 | 4.9 | 5.8 |
| MPEG12-*b*-PHpr10-*b*-PCL70 | 1/2 | 3.4 | 5.5 |
| MPEG12-*b*-PHpr10-*b*-PCL70 | 1/1 | 3.0 | 3.5 |
| MPEG12-*b*-PNZHpr10-*b*-PCL110 | 1/10 | 10.6 ± 0.45 | 2.0 ± 0.02 |
| MPEG12-*b*-PNZHpr10-*b*-PCL90 | 1/10 | 16.5 ± 0.58 | 2.1 ± 0.02 |
| MPEG12-*b*-PNZHpr10-*b*-PCL50 | 1/10 | 17.8 ± 0.65 | 2.2 ± 0.19 |
| MPEG12-*b*-PNZHpr10-*b*-PCL30 | 1/10 | 18.9 ± 0.72 | 2.7 ± 0.48 |

respect to drug-loading content. Drug-loading content increased with an increasing weight ratio of drug to the polymer for protected MPEG12-*b*-PNZHpr10-*b*-PCL70. Observations show contrary results for deprotected MPEG12-*b*-PHpr10-*b*-PCL70. The reason is rather complicated and can be affected by many factors, such as molecular weight, the ratio of hydrophobic segment to hydrophilic segment, crystallinity, and so on.[18] Until now, we did not know the reason clearly. A possible explanation is that a higher drug loading results in an increased drug concentration gradient between the polymer matrix and the other aqueous phase, which in turn leads to more drug loss in the fabrication process. The polymer itself may have a limited capacity to encapsulate a specific drug. Beyond its maximum capacity, more drugs might be washed during the fabrication process. As the feed weight ratio of AM to the polymer fixed at 0.1, drug entrapment efficiency and drug-loading content increased with decreasing length of the hydrophobic segment. This is because the shorter length of the hydrophobic segment in the core may have a larger capacity to encapsulate a drug.

## CONCLUSIONS

Starting from MPEG, this work obtains a novel triblock copolymer MPEG-*b*-PHpr-*b*-PCL by hydrogenolysis of MPEG-*b*-PNZHpr-*b*-PCL synthesized from the ROP of ε-CL with hydroxyl-terminated MPEG-*b*-PNZHpr-OH as a macroinitiator. This study investigated micellization behaviors of copolymer by fluorescence spectroscopy, DLS, and TEM. Fluorescence spectroscopy results confirmed that MPEG-*b*-PNZHpr-*b*-PCL easily forms micelles in aqueous solution and the deprotected copolymer MPEG-*b*-PHpr-*b*-PCL increases critical micelle concentration. The results of DLS and TEM show that the micelles of MPEG-*b*-PNZHpr-*b*-PCL and MPEG-*b*-PHpr-*b*-PCL exhibit a core-shell-corona and/or vesicle shape with unimodal distribution. Drug-loading content and drug entrapment efficiency mainly depend on copolymer composition and the feed weight ratio of AM to polymer. Drug release measurements are underway in our laboratory.

The authors are grateful to the proteomics core laboratory at Chang Gung University for the matrix-assisted laser desorption/ionization time-of-flight mass spectrometry analysis.

## References

1. Fustin, C. A.; Abetz, A.; Gohy, J. F. Eur Phys J E 2005, 16, 291.
2. Hadjichristidis, N.; Iatrou, H.; Pitsikalis, M.; Pispas, S.; Avgeropoulos, A. Prog Polym Sci 2005, 30, 725.
3. Huang, M. H.; Li, S.; Coudane, J.; Vert, M. Macromol Chem Phys 2003, 204, 1994.
4. Deng, C.; Chen, X.; Yu, H.; Sun, J.; Lu, T.; Jing, X. Polymer 2007, 48, 139.
5. Sun, J.; Deng, C.; Chen, X.; Yu, H.; Tian, H.; Sun, J.; Jing, X. Biomacromolecules 2007, 8, 1013.
6. Deng, C.; Tian, H.; Zhang, P.; Sun, J.; Chen, X.; Jing, X. Biomacromolecules 2006, 7, 590.
7. Deng, C.; Rong, G.; Tian, H.; Tang, Z.; Chen, X.; Jing, X. Polymer 2005, 46, 653.
8. Deng, M.; Wang, R.; Rong, G.; Sun, J.; Zhang, X.; Chen, X.; Jing, X. Biomaterials 2004, 25, 3553.
9. Tian, H. Y.; Deng, C.; Lin, H.; Sun, J.; Deng, M.; Chen, X.; Jing, X. Biomaterials 2005, 26, 4209.
10. Vivas, M.; Contreras, J.; López-Carrasquero, F.; Lorenzo, A. T.; Arnal, M. L.; Balsamo, V.; Müller, A. J.; Laredo, E.; Schmalz, H.; Abetz, V. Macromol Symp 2006, 239, 58.
11. Rzayev, J.; Hillmyer, M. A. Macromolecules 2005, 38, 3.
12. Lee, E. S.; Na, K.; Bae, Y. H. Nano Lett 2005, 5, 325.
13. Cate, M. G. J. ten; Börner, H. G. Macromol Chem Phys 2007, 208, 1437.
14. Lee, R. S.; Lin, Z. K.; Yang, J. M.; Lin, F. H. J Polym Sci Part A: Polym Chem 2006, 44, 4268.
15. Wilhelm, M.; Zhao, C. L.; Wang, Y.; Xu, R.; Winnik, A. Macromolecules 1991, 24, 1033.
16. Provencher, S. W.; Hendrix, J. J Chem Phys 1978, 69, 4273.
17. Zhou, J.; Takasu, A.; Ihai, Y.; Hirabayashi, T. Polym J 2004, 36, 182.
18. Hu, Y.; Jiang, X.; Ding, Y.; Zhang, L.; Yang, C.; Zhang, J.; Chen, J.; Yang, Y. Biomaterials 2003, 24, 2395.